

Synthesis, Structure and Magnetocaloric Properties of $\text{La}_{0.8}\text{K}_{0.15}\text{Li}_{0.05}\text{MnO}_3$ Perovskite Manganite



Y Regaieg^{1,2*}, W Cheikhrouhou-Koubaa¹, L Sicard³, M Koubaa^{1,4}, E K Hlil⁵ and A Cheikhrouhou¹

¹LT2S lab, Digital Research Center of Sfax, Sfax Technoparc, 3021 Sfax, Tunisia

²Faculty of Sciences of Gafsa, University of Gafsa, 2112 Gafsa, Tunisia

³ITODYS, Université Paris Diderot, UMR 7086 CNRS, 75205 Paris Cedex 13, France

⁴Institut Supérieur de Biotechnologie de Sfax, University of Sfax, 3000 Sfax, Tunisia

⁵Institut Néel, CNRS, Université Grenoble Alpes, 38042 Grenoble cedex 9, France

Submission: Febraury 27, 2023; **Published:** March 17, 2023

***Corresponding author:** Yassine Regaieg, Digital Research Center of Sfax, Sfax Technoparc, 3021 Sfax, Tunisia

Abstract

The synthesis, structural characterization, and magnetocaloric properties of $\text{La}_{0.8}\text{K}_{0.15}\text{Li}_{0.05}\text{MnO}_3$ perovskite manganite are reported. Our compound was synthesized using the sol-gel technique at low temperature. The Rietveld refinement of the X-ray powder diffraction shows that $\text{La}_{0.8}\text{K}_{0.15}\text{Li}_{0.05}\text{MnO}_3$ sample is single phase and crystallizes in a rhombohedral system with $R\bar{3}c$ space group. Paramagnetic-ferromagnetic phase transition at $T_c = 231.2$ K is observed for our studied compound. Magnetic entropy change, $-\Delta S_M$, deduced from isothermal magnetization curves, is about $2.39 \text{ J kg}^{-1} \text{ K}^{-1}$ in a magnetic field change of 5 T. The relative cooling power, RCP(S), value at 5 T reaches 272.4 J kg^{-1} . This value corresponds to about 66% of that observed in pure gadolinium.

Keywords: Manganites; Sol-gel Technique; X-ray Diffraction; Isothermal Magnetization; Magnetocaloric Effect; Stoichiometric

Introduction

Magnetic refrigeration (MR) based on the magnetocaloric effect (MCE) is a very promising technology to replace the traditional gas-compression refrigeration technology [1,2]. The MCE is an intrinsic property of magnetic materials and defined as the important change of temperature of an adiabatically isolated system with the application and removal of an external magnetic field [3-5]. The MCE is characterized by the magnetic entropy change, $-\Delta S_M$, and the adiabatic temperature change, ΔT_{ad} , under magnetic field changes. Mixed valence perovskite manganites with general formula $\text{Ln}_{1-x}\text{X}_x\text{MnO}_3$, where Ln is a trivalent rare-earth ion and X a monovalent alkaline or divalent alkaline-earth ion, are typical MCE materials and have been extensively studied these last years in view of their fascinating properties arising from spin-balance sensitivity, orbital contribution, lattice distortion, charge degrees of freedom [6,7]. Monovalent substituted perovskite manganites which are known to introduce large potential fluctuations are typical materials that have been reported [8-10]. Among the evaluated manganites, a family of $\text{Ln}_{1-x}\text{X}_x\text{MnO}_3$ appear as very promising candidates for the desired application. In this context, the main objective of our work is to enhance the MCE of $\text{La}_{0.8}\text{K}_{0.2}\text{MnO}_3$ with Li substitution. Therefore, in this pa-

per, we investigate the structural, magnetic and magnetocaloric properties of $\text{La}_{0.8}\text{K}_{0.15}\text{Li}_{0.05}\text{MnO}_3$ compound synthesized using the sol-gel technique at low temperature.

Experimental Techniques

$\text{La}_{0.8}\text{K}_{0.15}\text{Li}_{0.05}\text{MnO}_3$ sample were prepared by the sol-gel technique (Pechini method) at low temperature [11]. The stoichiometric amounts of La_2O_3 , K_2CO_3 , Li_2CO_3 and MnO_2 with high purity (Sigma Aldrich 99.9%) were dissolved in concentrated nitric acid to transform them into nitrates. This step was carried out at 60°C in order to accelerate the dissolution. After total dissolution, citric acid, a compliant agent, and ethylene glycol, a polymerization agent, were added. This solution is slowly evaporated at 130°C until the formation of a residue of high viscosity. A transparent gel is developed during the heating process. The temperature was subsequently raised at $10^\circ\text{C min}^{-1}$ rate up to 300°C to assure the propagation of a combustion, which transforms the gel into a fine powder. The resulting powder is heated at 450°C during 6 hours in order to decompose the organics. After crushing, the sample was calcined at 650°C during 12 hours and then at 800°C for the same duration with intermediate grinding. Finally, the powder was then pressed into pellets (of about 1 mm thickness and 10

mm diameter) and sintered at 900°C during 24 hours. All annealings are performed in air.

The crystallographic structure was determined by powder X-ray diffraction (XRD) at room temperature using a Panalytical diffractometer (Empyrean model). Structural analysis was carried out using the standard Rietveld technique [12]. The microstructure was studied by Scanning Electron Microscopy (SEM) using a *Supra40* ZEISS FEG-SEM microscope operating at 10 kV.

Magnetization measurements versus temperature in the range of 5-400K and versus magnetic applied field in the 0-5 T range were carried out using a MPMS-XL Quantum Design SQUID magnetometer. The magnetocaloric effect (MCE) was determined from the magnetization measurements versus magnetic applied field at several temperatures.

Results and Discussion

The powder X-ray diffraction pattern of the $\text{La}_{0.8}\text{K}_{0.15}\text{Li}_{0.05}\text{MnO}_3$ compound synthesized, recorded at room temperature, along with Rietveld refinement is shown in (Figure 1). The diffraction peaks can be indexed in the rhombohedral system with $R\bar{3}c$ space group. The quality factors indicating the agreement between the observed and the calculated profiles are $R_b = 2.58$, $R_p = 16.1$ and $\chi^2 = 3.13$. The corresponding lattice parameters and unit cell volume are $a = b = 5.511(2)$ Å, $c = 13.378(4)$ Å and $V = 351.90$ Å³. We have also calculated the Mn-O bond length and the Mn-Mn bond angle from the position of the ions in the unit cell and lattice parameters, which are found to be 1.961(4) Å and 164.14(3)° respectively. A SEM image of the $\text{La}_{0.8}\text{K}_{0.15}\text{Li}_{0.05}\text{MnO}_3$ sample is shown in (Figure 2). The almost polygonal grains have an average size in the submicrometer range.

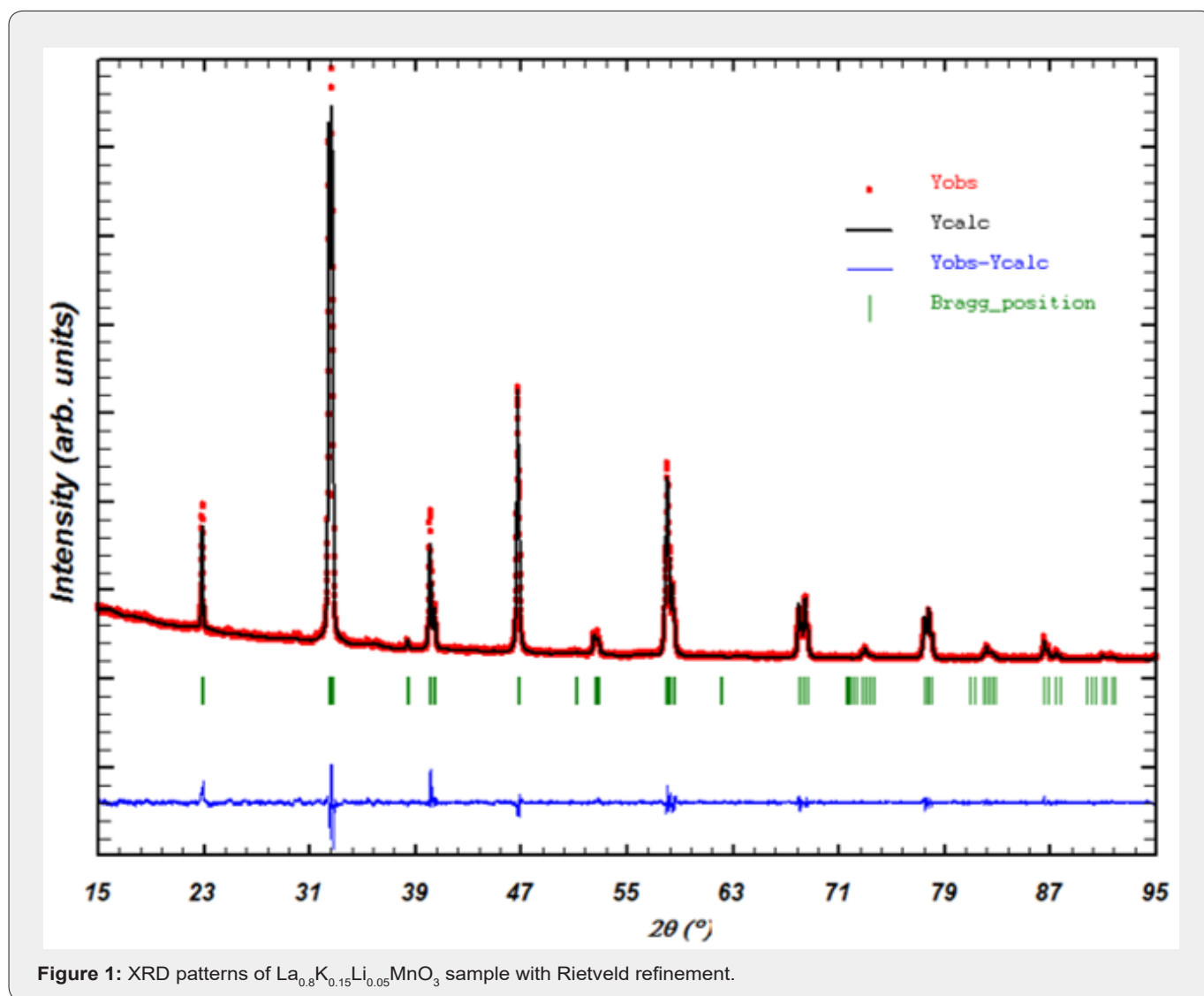


Figure 1: XRD patterns of $\text{La}_{0.8}\text{K}_{0.15}\text{Li}_{0.05}\text{MnO}_3$ sample with Rietveld refinement.

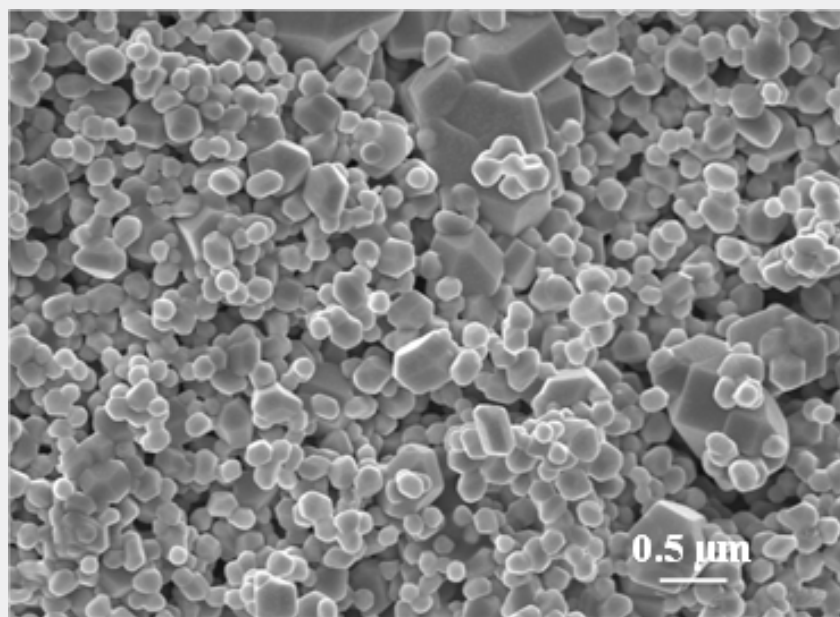


Figure 2: SEM image of the $\text{La}_{0.8}\text{K}_{0.15}\text{Li}_{0.05}\text{MnO}_3$ compound.

Magnetization measurements as a function of temperature, $M(T)$, were plotted in the 5-400 K range for $\text{La}_{0.8}\text{K}_{0.15}\text{Li}_{0.05}\text{MnO}_3$ ($0 \leq x \leq 0.075$) compound by applying a magnetic field of 50 mT (Figure 3). Our sample exhibited a paramagnetic to ferromagnetic

transition with decreasing temperature. The Curie temperature, T_c (defined as the temperature at which dM/dT shows a minimum), is found to be 231.2 K.

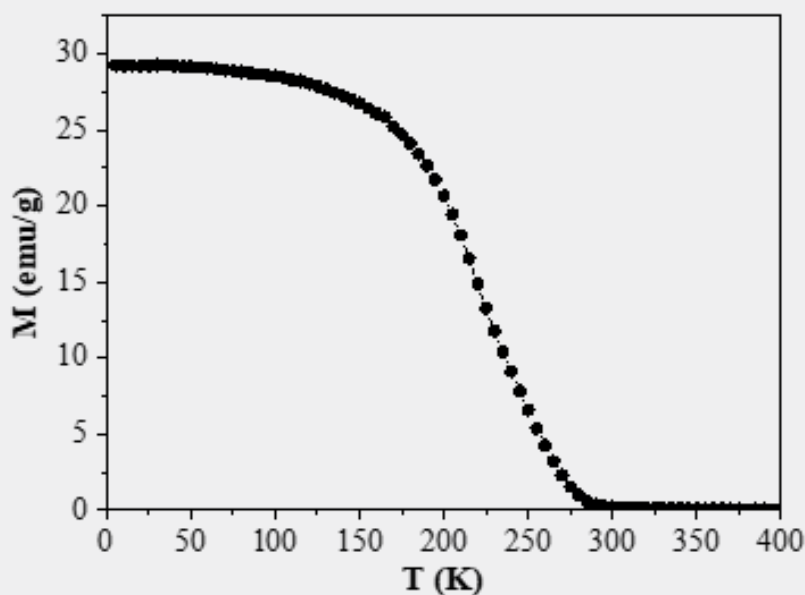


Figure 3: Temperature dependence of the magnetization of $\text{La}_{0.8}\text{K}_{0.15}\text{Li}_{0.05}\text{MnO}_3$ sample at 0.05 T.

The Curie-Weiss analysis of the data above T_c resulted in effective paramagnetic moment μ_{eff}^{exp} of $4.91 \mu_B$ higher than the theoretical value $\mu_{eff}^{the} = 4.52 \mu_B$.

The magnetization versus magnetic field, $M(H)$, up to 5 T at

different temperatures in the 160-330 K range was also measured for $\text{La}_{0.8}\text{K}_{0.15}\text{Li}_{0.05}\text{MnO}_3$ sample (Figure4(a)). Below T_c , the magnetization increases sharply below 0.5 T and tends to saturation for higher magnetic fields, which confirms the ferromagnetic behavior of our synthesized sample at low temperatures.

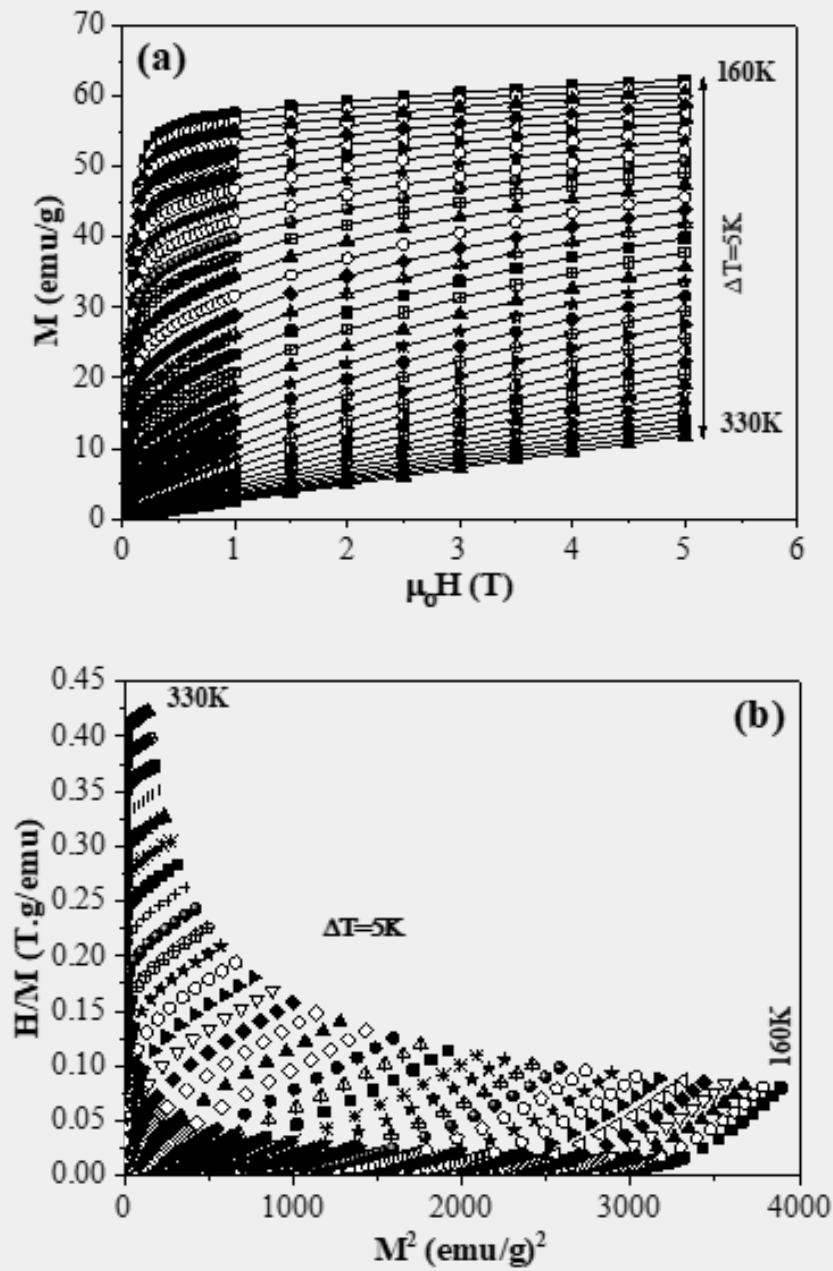


Figure 4: (a) Variation of the magnetization as a function of applied magnetic field at different temperatures and (b) H/M versus M^2 isotherms for $\text{La}_{0.8}\text{K}_{0.15}\text{Li}_{0.05}\text{MnO}_3$ sample.

We plot in (Figure4(b)) the Arrott curves, H/M versus M^2 , deduced from $M(H)$ for $\text{La}_{0.8}\text{K}_{0.15}\text{Li}_{0.05}\text{MnO}_3$ sample. The plots show a positive slope, above T_c , which indicates that a second order ferromagnetic to paramagnetic phase transition occurs [13]. Furthermore, the T_c values deduced from these plots are very close to those determined from $M(T)$.

The magnetic entropy change, $-\Delta S_M$, induced by the magnetic field change, ΔH , was determined using the $M(H)$ curves. According to the classical thermodynamic theory based on Maxwell relations, $-\Delta S_M$, can be evaluated through the formula:

$$\Delta S_M(T, H) = S_M(T, H) - S_M(T, 0) = \int_0^{\mu_0 H_{\max}} \mu_0 \left(\frac{\partial M}{\partial T} \right)_H dH \quad (1)$$

where $\mu_0 H_{\max}$ is the maximal value of the magnetic applied field. In practice the relation is approximated as:

$$-\Delta S_M = \sum_i \frac{M_i - M_{i+1}}{T_{i+1} - T_i} \Delta H_i \quad (2)$$

where M_i and M_{i+1} are the experimental values of magnetization measured at temperatures T_i and T_{i+1} , respectively, under magnetic applied field H_i [14, 15]. (Figure 5) shows the temperature dependence of the $-\Delta S_M$ under different magnetic field change for $\text{La}_{0.8}\text{K}_{0.15}\text{Li}_{0.05}\text{MnO}_3$ sample. $|\Delta S_M|$ increases with increasing

magnetic applied field change. The maximum values of the magnetic entropy change $|\Delta S_M^{Max}|$ observed around T_C are equal to 0.55, 1.08, 1.56, 1.99 and 2.39 $\text{J kg}^{-1} \text{K}^{-1}$ for magnetic field changes of 1, 2, 3, 4 and 5 T respectively.

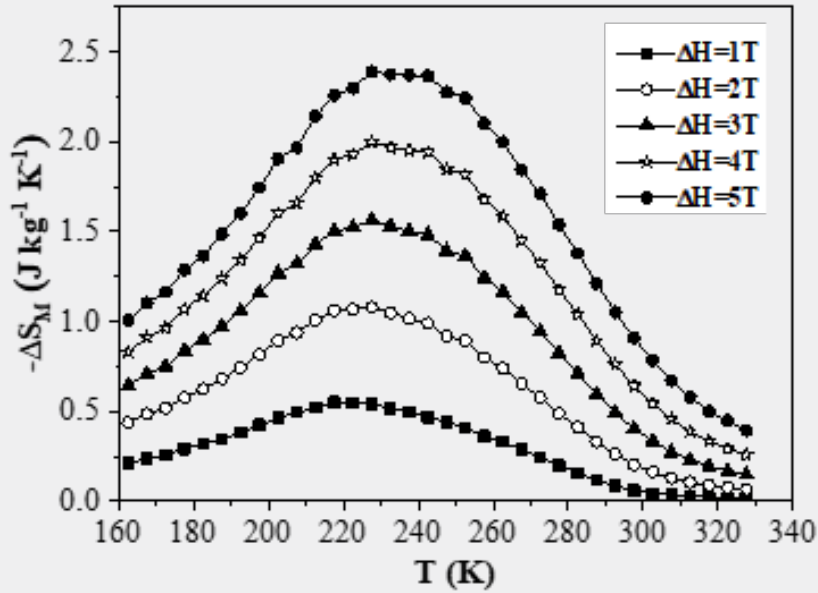


Figure 5: Magnetic entropy change, $-\Delta S_M$, versus temperature at different magnetic field changes for $\text{La}_{0.8}\text{K}_{0.15}\text{Li}_{0.05}\text{MnO}_3$ compound.

The variation of the maximum of the magnetic entropy change as a function of the magnetic field change, for the $\text{La}_{0.8}\text{K}_{0.15}\text{Li}_{0.05}\text{MnO}_3$ sample, exhibits a monotone increase, as shown in (Figure 6(a)), which corresponds to the magnetic transition from

ferromagnetic to paramagnetic states. In accordance to Oesterreicher *et al.* [16], the field dependence of the magnetic entropy change at T_C of materials with a second order phase transition can be described by a power law of the type [17]:

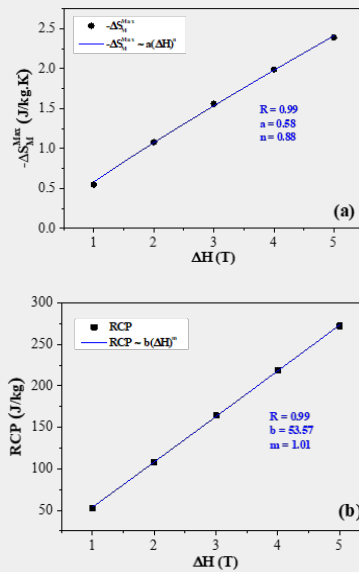


Figure 6: Field dependence of $-\Delta S_M^{Max}$ (a) and RCP (b) for $\text{La}_{0.8}\text{K}_{0.15}\text{Li}_{0.05}\text{MnO}_3$ sample.

$$-\Delta S_M^{Max} \approx a(\Delta H)^n \quad (3)$$

where a is a constant and the exponent n depends up on the magnetic state of the sample. The obtained value of n is 0.88, which is significantly different than $2/3$, as predicted by the mean field model [17]. The deviation from $n = 2/3$ is due to the presence of local magnetic inhomogeneities in the vicinity of transition temperature [18]. This result is similar to those obtained for other manganites system [19-21].

In magnetic refrigeration technology, it is important that the magnetocaloric effect extends over a large temperature range. The relative cooling power (RCP(S)) is evaluated as $RCP(S) = -\Delta S_M^{Max}(T, \Delta H) * \delta T_{FWHM}$ where δT_{FWHM} is the full-width at half-maximum of $|\Delta S_M|$ versus temperature curve [22]. We plot in (Figure 6(b)) the RCP values as a function of the magnetic field

change, ΔH . It can be observed that the RCP values increase with ΔH indicating that RCP is strong field dependent. Indeed, RCP can be approximately expressed as a power law:

$$RCP \approx b(\Delta H)^m \quad (4)$$

where m is the critical exponent of the magnetic transition. RCP should scale with field as a power law with an exponent m . The fitting value of m is found to be 1.01 for our sample. This m result is comparable with values previous studies [21,23,24]. (Table 1) shows the obtained results in comparison with those of several magnetic materials that could be used as active refrigerants taken from the literature. It is clear from the table that the obtained values are larger than the parent compound $La_{0.8}K_{0.15}Li_{0.05}MnO_3$ [8]. On the other hand, our RCP(S) represents about 66% of the prototype magnetic refrigerant material Gd RCP value (410 J/kg [28]) for a magnetic field change of 5T.

Table 1: Curie temperature T_C , magnetic field change ΔH , maximum of the magnetic entropy change $-\Delta S_M^{Max}$ and RCP values for $La_{0.8}K_{0.15}Li_{0.05}MnO_3$ sample compared to values reported in the literature.

Sample	T_C (K)	ΔH (T)	$-\Delta S_M^{Max}$ (J/kgK)	RCP (J/kg)	Reference
$La_{0.8}K_{0.15}Li_{0.05}MnO_3$	231.2	1	0.55	51.9	Present work
		2	1.08	107.9	
		3	1.56	164.3	
		5	2.39	272.4	
$Pr_{0.8}Na_{0.2}MnO_3$	92	2	2.48	101.5	[25]
$La_{0.65}Dy_{0.05}Sr_{0.3}MnO_3$	265	2	0.86	80	[26]
$La_{0.8}K_{0.2}MnO_3$	330	5	3.48	201.7	[8]
$La_{0.8}Na_{0.2}MnO_3$	330	5	4.23	228.6	[8]
$La_{0.8}Ag_{0.2}MnO_3$	278.5	5	6.12	217.8	[27]
$La_{0.8}Ag_{0.15}K_{0.05}MnO_3$	300	5	5.28	222.3	[27]
Gd	294	5	10.2	410	[28]

Conclusion

In summary, the polycrystalline $La_{0.8}K_{0.15}Li_{0.05}MnO_3$ sample was prepared by the sol-gel technique at low temperature. Our compound crystallizes in the rhombohedral system with $R\bar{3}c$ space group. Magnetic measurements revealed that our sample manganite undergoes a second order magnetic transition with the paramagnetic-ferromagnetic transition at a $T_C \sim 231.2$ K. The maximum of the magnetic entropy change, $|\Delta S_M^{Max}|$, and the relative cooling power, RCP(S), associated with the transition are found to be $2.39 \text{ J kg}^{-1} \text{ K}^{-1}$ and 272.4 J kg^{-1} respectively, under a magnetic field change of 5T. These results suggest that our synthesized sample could be used as an active magnetic refrigerant working below room temperature..

Acknowledgment

This study has been supported by the Tunisian Ministry of Higher Education and Scientific Research.

References

- Glanz J (1998) Making a Bigger Chill With Magnets, Science 279(5359): 2045.
- Zimm C, Jastrab A, Sternberg A, Pecharsky VK, Gschneidner KA, et al. (1998) Description and Performance of a Near-Room Temperature Magnetic Refrigerator. Adv Cryog Eng 43: 1759-1766.
- Casanova F, Batlle X, Labarta A (2002) Scaling of the entropy change at the magnetoelastic transition in $Gd_5(Si_xGe_{1-x})_4$. Phys Rev B 66: 212402-212405.
- Zhang XY, Chen Y, Li ZY (2007) Large magnetocaloric effect in chromium dioxide with second-order phase transition. J Phys D Appl Phys 40: 3243.
- Tishin AM, Spichkin YI (2013) The Magnetocaloric Effect and its Applications. Institute of Physics Publishing.
- Al-Yahmadi IZ, Gismelseed AM, Al Ma Mari F, Al-Rawas AD, Al-Harhi SH, et al. (2021) Structural, magnetic and magnetocaloric effect studies of $Nd_{0.6}Sr_{0.4-x}Mn_{1-x}O_3$ (A=Co, Ni, Zn) perovskite manganites. J Alloys Compd 875: 159977.
- Regaieg Y, Ayadi F, Monnier J, Reguer S, Koubaa M, et al. (2014) Magnetocaloric properties of $La_{0.67}Ca_{0.33}MnO_3$ produced by reactive spark plasma sintering and by conventional ceramic route. Mater Res Express 1: 046105-046118.
- Regaieg Y, Koubaa M, Cheikhrouhou Koubaa W, Cheikhrouhou A, Mhiri T (2010) Magnetocaloric effect above room temperature in the K-doped $La_{0.8}Na_{0.2-x}K_xMnO_3$ manganites. J Alloys Compd 502: 270-274.
- Ben Rejeb M, Ben Osman C, Regaieg Y, Marzouki-Ajmi A,

- Cheikhrouhou-Koubaa W, et al. (2017) A comparative study of $\text{La}_{0.65}\text{Ca}_{0.2}(\text{Na}_{0.5}\text{K}_{0.5})_{0.15}\text{MnO}_3$ compound synthesized by solid-state and sol-gel process. *J Alloys Comp* 695: 2597-2604.
10. Phan MH, Yu SC (2007) Review of the magnetocaloric effect in manganite materials. *J Magn Magn Mater* 308: 325-340.
 11. Ayadi F, Cheikhrouhou-Koubaa W, Koubaa M, Nowak S, Sicard L, et al. (2014) Effect of synthesis method on structural, magnetic and magnetocaloric properties of $\text{La}_{0.7}\text{Sr}_{0.2}\text{Ag}_{0.1}\text{MnO}_3$ manganite. *Mater Chem Phys* 145: 56-59.
 12. Rietveld HM (1969) A profile refinement method for nuclear and magnetic structures. *J Appl Crystallogr* 2: 65-71.
 13. Banerjee SK (1964) On a generalised approach to first and second order magnetic transitions. *Phys Lett* 12: 16-17.
 14. Dinesen AR, Linderoth S, Moerup S (2005) Direct and indirect measurement of the magnetocaloric effect in $\text{La}_{0.67}\text{Ca}_{0.33-x}\text{Sr}_x\text{MnO}_3$ ($x \in [0; 0.33]$). *J Phys Condens Matter* 17: 6257-6269.
 15. McMichael RD, Ritter JJ, Shull RD (1993) Enhanced magnetocaloric effect in $\text{Gd}_3\text{Ga}_{5-x}\text{Fe}_x\text{O}_{12}$. *J Appl Phys* 73: 6946-6948.
 16. Oesterreicher H, Parker FT (1984) Magnetic cooling near Curie temperatures above 300 K. *J Appl Phys* 55: 4334.
 17. Franco V, Conde A (2010) Scaling laws for the magnetocaloric effect in second order phase transitions: From physics to applications for the characterization of materials. *Int J Refrig* 33: 465-473.
 18. Franco V, Blázquez JS, Conde A (2006) The influence of Co addition on the magnetocaloric effect of Nanoperm-type amorphous alloys. *J Appl Phys* 100: 064307.
 19. Reshmi CP, Savitha Pillai S, Suresh KG, Varma MR (2013) Room temperature magnetocaloric properties of Ni substituted $\text{La}_{0.67}\text{Sr}_{0.33}\text{MnO}_3$. *Solid State Sci* 19: 130-135.
 20. Phan TL, Zhang P, Thanh TD, Yu SC (2014) Crossover from first-order to second-order phase transitions and magnetocaloric effect in $\text{La}_{0.7}\text{Ca}_{0.3}\text{Mn}_{0.91}\text{Ni}_{0.09}\text{O}_3$. *J Appl Phys* 115: 17A912.
 21. Kharrat N, Sfirir Debbabi I, Cheikhrouhou-Koubaa W, Koubaa M, Cheikhrouhou A, et al. (2019) Magnetocaloric Effect in $\text{La}_{0.67}\text{Ba}_{0.33}\text{Mn}_{0.95}\text{Ni}_{0.05}\text{O}_3$ Manganite Near Room Temperature. *J Supercond Nov Magn* 32: 1241-1251.
 22. Gschneidner KA, Pecharsky VK (2000) Magnetocaloric Materials. *Annu Rev Mater Sci* 30: 387-429.
 23. Ezaami A, Sellami-Jmal E, Cheikhrouhou-Koubaa W, Koubaa M, Cheikhrouhou A (2017) Phenomenological model of magnetocaloric effect in $\text{La}_{0.7}\text{Ca}_{0.2}\text{Ba}_{0.1}\text{MnO}_3$ manganite around room temperature. *J Supercond Nov Magn* 30: 911-916.
 24. Ben Khelifa H, M'nassri R, Cheikhrouhou-Koubaa W, Schmerber G, Leuvrey C, et al. (2017) Structural characterization and magnetic field dependence of the magnetocaloric properties in $\text{Pr}_{0.8}\text{Na}_{0.05}\text{K}_{0.15}\text{MnO}_3$ ceramic. *J Magn Magn Mater* 439: 148-155.
 25. Ben Khelifa H, Regaieg Y, Cheikhrouhou-Koubaa W, Koubaa M, Cheikhrouhou A (2015) Structural magnetic and magnetocaloric properties of K-doped $\text{Pr}_{0.8}\text{Na}_{0.2-x}\text{K}_x\text{MnO}_3$ manganites. *J Alloy Compd* 650: 676-683.
 26. Felhi R, Koubaa M, Cheikhrouhou-Koubaa W, Cheikhrouhou A (2017) Structural, magnetic, magnetocaloric and critical behavior investigations of $\text{La}_{0.65}\text{Dy}_{0.05}\text{Sr}_{0.3}\text{MnO}_3$ manganite. *J Alloys Compd* 726: 1236-1245.
 27. Regaieg Y, Koubaa M, Cheikhrouhou-Koubaa W, Cheikhrouhou A, Sicard L, et al. (2012) Structure and magnetocaloric properties of $\text{La}_{0.8}\text{Ag}_{0.2-x}\text{K}_x\text{MnO}_3$ perovskite manganites. *Mater Chem Phys* 132: 839-845.
 28. Gschneider KA, Pecharsky VK, Tsokol AO (2005) Recent developments in magnetocaloric materials. *Rep Prog Phys* 68: 1479-1539.



This work is licensed under Creative Commons Attribution 4.0 License
DOI: [10.19080/CTBEB.2023.21.556061](https://doi.org/10.19080/CTBEB.2023.21.556061)

**Your next submission with Juniper Publishers
will reach you the below assets**

- Quality Editorial service
- Swift Peer Review
- Reprints availability
- E-prints Service
- Manuscript Podcast for convenient understanding
- Global attainment for your research
- Manuscript accessibility in different formats
(Pdf, E-pub, Full Text, Audio)

• Unceasing customer service

Track the below URL for one-step submission

<https://juniperpublishers.com/online-submission.php>